

# Unusually Large Young's Moduli of Amino Acid Molecular Crystals

Ido Azuri, Elena Meirzadeh, David Ehre, Sidney R. Cohen, Andrew M. Rappe, Meir Lahav, Igor Lubomirsky,\* and Leeor Kronik\*

**Abstract:** Young's moduli of selected amino acid molecular crystals were studied both experimentally and computationally using nanoindentation and dispersion-corrected density functional theory. The Young modulus is found to be strongly facet-dependent, with some facets exhibiting exceptionally high values (as large as 44 GPa). The magnitude of Young's modulus is strongly correlated with the relative orientation between the underlying hydrogen-bonding network and the measured facet. Furthermore, we show computationally that the Young modulus can be as large as 70–90 GPa if facets perpendicular to the primary direction of the hydrogen-bonding network can be stabilized. This value is remarkably high for a molecular solid and suggests the design of hydrogen-bond networks as a route for rational design of ultra-stiff molecular solids.

In recent years, there has been growing interest in the mechanical properties of molecular solids,<sup>[1–9]</sup> often deduced from nanoindentation experiments.<sup>[10–13]</sup> Partly, this interest is driven by practical issues, as mechanical considerations affect the stability of molecular solids across a diverse range of applications, from pharmaceuticals<sup>[3,14–16]</sup> to energetic materials.<sup>[4,5]</sup> But the research is also driven by basic science, as some molecular solids exhibit Young's moduli much higher than that expected from naive considerations.<sup>[1,2,17]</sup>

Recent theoretical work has suggested that the enhanced stiffness of molecular-solid-based materials, such as diphenylalanine-based materials, arises from a particular crystalline arrangement featuring a preponderance of inter-molecular van-der-Waals interactions that help stabilize a solid comprised of tube-like structures.<sup>[17]</sup> It therefore stands to reason that equally high, or even higher yet, Young's moduli could be obtained from crystals that also possess significant inter-molecular hydrogen bonds. Indeed, this is hinted at by the

report of a reduced elastic modulus of about 16–21 GPa for the energetic molecular solid, cyclotrimethylene trinitramine (RDX),<sup>[4,5]</sup> and elastic moduli exceeding 30 GPa for the sucrose molecular solid,<sup>[18]</sup> but no direct link to the hydrogen-bonding network is established.

A simple yet important class of molecular solids in which this issue can be assessed unequivocally and quantitatively is the amino acid crystals. However, to the best of our knowledge, little work along these lines has been performed. Early work<sup>[19]</sup> has reported Young's moduli for several amino acid crystals, but directional measurements were not reported, and relatively small values were found. More recent work appears to support the hypothesis of large Young's moduli indirectly: the bulk moduli of various amino acid crystals were deduced from high pressure measurements,<sup>[20–26]</sup> and relatively high values were found. Also the microhardness of L-serine<sup>[27]</sup> and L-phenylalanine benzoic acid<sup>[28]</sup> was determined to be comparable to that of hard matter. Still, we are not aware of direct studies, either experimental or theoretical, showing high Young's moduli for amino-acid crystals. Even more importantly, the specific role that hydrogen-bonding plays in the mechanical properties of amino acid crystals, including their possible directionality, has not been elucidated.

Herein, we report a combined experimental and computational study of Young's moduli in five prototypical amino acid molecular crystals:  $\alpha$ -glycine,  $\gamma$ -glycine, L-alanine, DL-serine, and glycylglycine (Figure 1). These were chosen because they all exhibit the same zwitterionic group, yet their packing arrangements offer a rich variety of directionality and hydrogen-bonding scenarios. In particular, we investigate the directional dependence of Young's modulus. We find Young's modulus to be strongly facet-dependent. Some experimentally accessible facets exhibit exceptionally high values (as large as 44 GPa) and other, presently inaccessible facets are predicted to exhibit values as high as 90 GPa. These findings are rationalized in terms of the underlying hydrogen-bonding network and its orientation with respect to the measured facet, opening the door to rational design of ultra-stiff molecular solids.

Young's modulus along a specific axis is defined as the ratio between the applied stress and the resulting strain along that axis, within the elasticity limit. Young's moduli, obtained from nanoindentation experiments (see Methods Section for details) for the five amino acid crystals examined in this work, are given in Table 1. Two important observations stand out; First, Young's moduli are very large across the board: the smallest measured value is more than 20 GPa and the largest one is 44 GPa. These values should be compared to Young's moduli of 1–15 GPa for many molecular solids.<sup>[29–32]</sup> Second, for the two crystals where a Young's modulus could be measured for different crystal faces ( $\alpha$ -glycine and L-alanine),

[\*] I. Azuri,<sup>[†]</sup> E. Meirzadeh,<sup>[†]</sup> Dr. D. Ehre, Prof. M. Lahav, Prof. I. Lubomirsky, Prof. L. Kronik  
Department of Materials and Interfaces,  
Weizmann Institute of Science  
Rehovoth 76100 (Israel)  
E-mail: Igor.Lubomirsky@weizmann.ac.il  
leeor.kronik@weizmann.ac.il

Dr. S. R. Cohen  
Chemical Research Support, Weizmann Institute of Science  
Rehovoth 76100 (Israel)

Prof. A. M. Rappe  
The Makineni Theoretical Laboratories, Department of Chemistry,  
University of Pennsylvania  
Philadelphia, PA 19104-6323 (USA)

[†] These authors contributed equally to this work.

Supporting information for this article is available on the WWW under <http://dx.doi.org/10.1002/anie.201505813>.

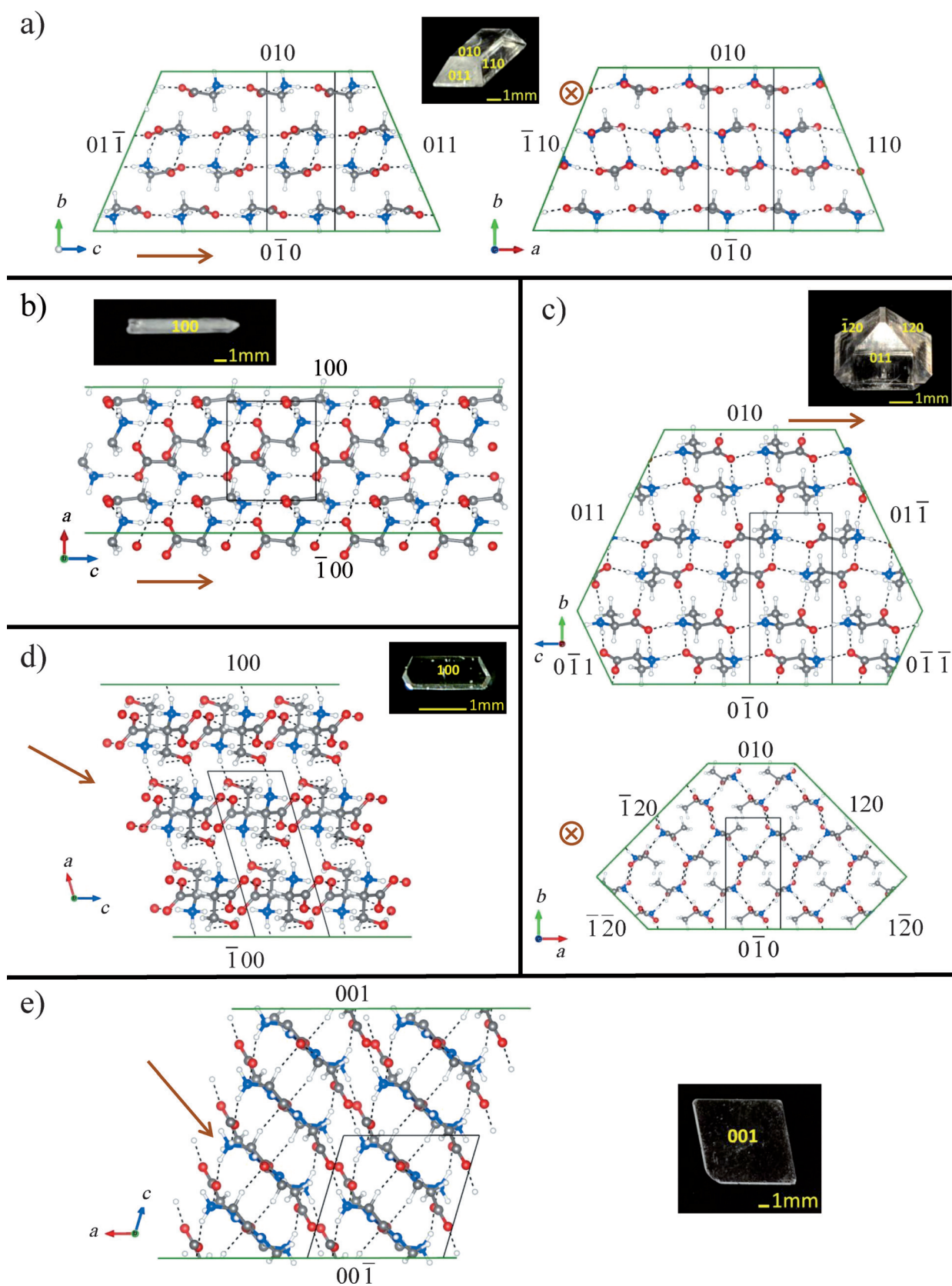


**Figure 1.** Schematic view of various projections of the crystalline structure of a)  $\alpha$ -glycine, b)  $\gamma$ -glycine, c) L-alanine, d) DL-serine, and e) glycyglycine. For each, a picture of the crystal, with the crystalline faces marked, is given as an inset. Hydrogen bonds are depicted by dashed lines. The direction of maximum stiffness, in the  $c$  direction for cases (a)–(c), in the  $ac$  plane for cases (d)–(e), is denoted by a brown solid arrow. Carbon, oxygen, nitrogen, and hydrogen atoms are shown in gray, red, blue, and white, respectively.

**Table 1:** Measured and calculated Young's moduli (in GPa, with the uncertainty representing the standard deviation), obtained for five amino-acid crystals along specific crystallographic directions (given in parentheses), as well as computed minimal and maximal Young's moduli. The direction of the maximal Young modulus is indicated in Figure 1, and the complete distribution of Young modulus values is given in Figure 2.

Material	Method	Crystallographic Face	min	max
$\alpha$ -glycine	Exp	$26 \pm 1$ (010); $29 \pm 2$ (110); $33 \pm 1$ (011); $44 \pm 1$ (001)		
	Theo	29 (010); 32 (110); 41 (011); 57 (001)	26	94
$\gamma$ -glycine	Exp	$28 \pm 1$ (100)		
	Theo	19 (100)	19	75
L-alanine	Exp	$21.2 \pm 0.3$ (010); $20.8 \pm 0.4$ (120); $34.4 \pm 0.2$ (011)		
	Theo	19 (010); 27 (120); 34 (011)	15	68
DL-serine	Exp	$23.1 \pm 0.5$ (100)		
	Theo	24 (100)	11	31
glycylglycine	Exp	$26 \pm 2$ (001)		
	Theo	21 (001)	14	91

the results are strongly facet-dependent: variance up to 70 % for  $\alpha$ -glycine and 65 % for L-alanine.

To gain insight into these results, we performed first-principles calculations of the elastic constants, based on dispersion-corrected density functional theory (DFT; Methods section). In this approach, conventional DFT approximations, which do not (or only barely) capture dispersive interactions, are augmented by pairwise interatomic terms that are damped at short range. This preserves the successful description of strong (ionic, covalent) bonds, but adds the missing long-range dispersion that is essential for hydrogen-bond and van der Waals interactions.<sup>[33–35]</sup> Such corrections have been shown to be highly successful for molecular solids in general and for their response properties in particular.<sup>[36]</sup>

A prerequisite for predicting response properties accurately is the attainment of accurate equilibrium structural parameters. Although the DFT calculations are performed at 0 K, comparison to structural data obtained at room temperature is meaningful, owing to the relatively small thermal expansion coefficients of the amino acid crystals studied herein.<sup>[37,38]</sup> The computed equilibrium geometries were found to be in very good agreement with the experimental values, with an absolute average error in lattice parameters of < 0.7 % for all structures studied (Supporting Information).

The structural accuracy allows us to compute Young's moduli explicitly, for an arbitrary direction.<sup>[39–41]</sup> This is based on the calculation of a frozen-nuclei elastic tensor from stress-strain relations<sup>[42]</sup> augmented with corrections for the force-response internal-strain tensor (see the Supporting Information for full details and for validation against calculations of elastic constants from energy-strain and stress-strain curves).<sup>[43]</sup> The computed Young's moduli obtained along the experimentally accessible crystallographic directions, as well as the minimum and maximum values, are given in Table 1. Three-dimensional renderings of the anisotropy of Young's moduli<sup>[41,14]</sup> are given in Figure 2.

Analysis of the computational data leads to two important observations. First, the agreement between theory and experiment is excellent in most cases (deviations of the order of  $\leq 10\%$ , often on par with the experimental accuracy), but in some cases larger deviations are found, notably around 20 % for glycylglycine and around 32 % for  $\gamma$ -glycine. Even with these larger deviations taken into account, the computational results agree fully with the experimental results in predicting the unusually large values of Young's moduli, their overall range, and the strong facet dependence. Even more importantly, Figure 2 reveals that for all cases, except DL-serine, there is a very high degree of anisotropy in the Young's modulus. In fact, the results suggest that Young's moduli range between minimum values of the order of 10–20 GPa to extremely high maximal values of the order of 70–90 GPa. Actual observation of such high values would necessitate the stabilization of an appropriately oriented surface, which is not always achievable experimentally. Still, the highest value obtained (44 GPa for  $\alpha$ -glycine) was measured along the (001) face, which is not a natural cleavage plane but instead was obtained by polishing. Nevertheless, our findings show that the potential stiffness of amino acid based crystals has not been fully exploited yet.

What dominates the unusual stiffness of these systems? Careful comparison of Young's modulus anisotropy given in Figure 2 with the detailed crystallographic directions given in Figure 1 suggests that  $-\text{NH}_3^+\cdots\text{O}-$  intermolecular hydrogen bonds strongly contribute to the stiffness, as maximal Young's modulus values are obtained when pressure is applied along the overall direction of such hydrogen-bond networks. For example, for  $\alpha$ -glycine the maximal Young's modulus is found along the *c* direction, which is the direction of the strongest hydrogen-bond network, with secondary locally maximal Young modulus values found close to the weaker hydrogen-bond networks along the *a* and *b* directions. A similar picture of global and local maxima obtained along the stronger and weaker hydrogen-bond network directions is found for glycylglycine. Lower moduli, which are still quite high for organic materials, are obtained for the natural crystallographic faces (Table 1). This is because the pressure applied is either not directly along the hydrogen bond direction or because the structures along these directions exhibit structural (crystallographic) voids, which soften the material (see, for example, the voids inside the unit cell of Figure 1 c).

As shown in Figure 2, DL-serine is exceptional in the sense that its highest computed Young's modulus, 31 GPa, is substantially smaller than the maximal Young's moduli computed for the other crystals and that its anisotropy is much smaller. Two factors can explain this observation. First, it exhibits relatively large voids in all planes. Second, this crystal contains, in combination with the zwitterionic bonds along some directions, much weaker hydrogen bonds from the alcohol group of the serine molecule.

In conclusion, we have performed a combined experimental and computational study of prototypical amino acid crystals. Experimentally, we find Young's modulus values as high as 44 GPa, which are exceptionally large for such simple molecular solids. Theoretically, we have confirmed these values and explained them in terms of a dominant contribu-

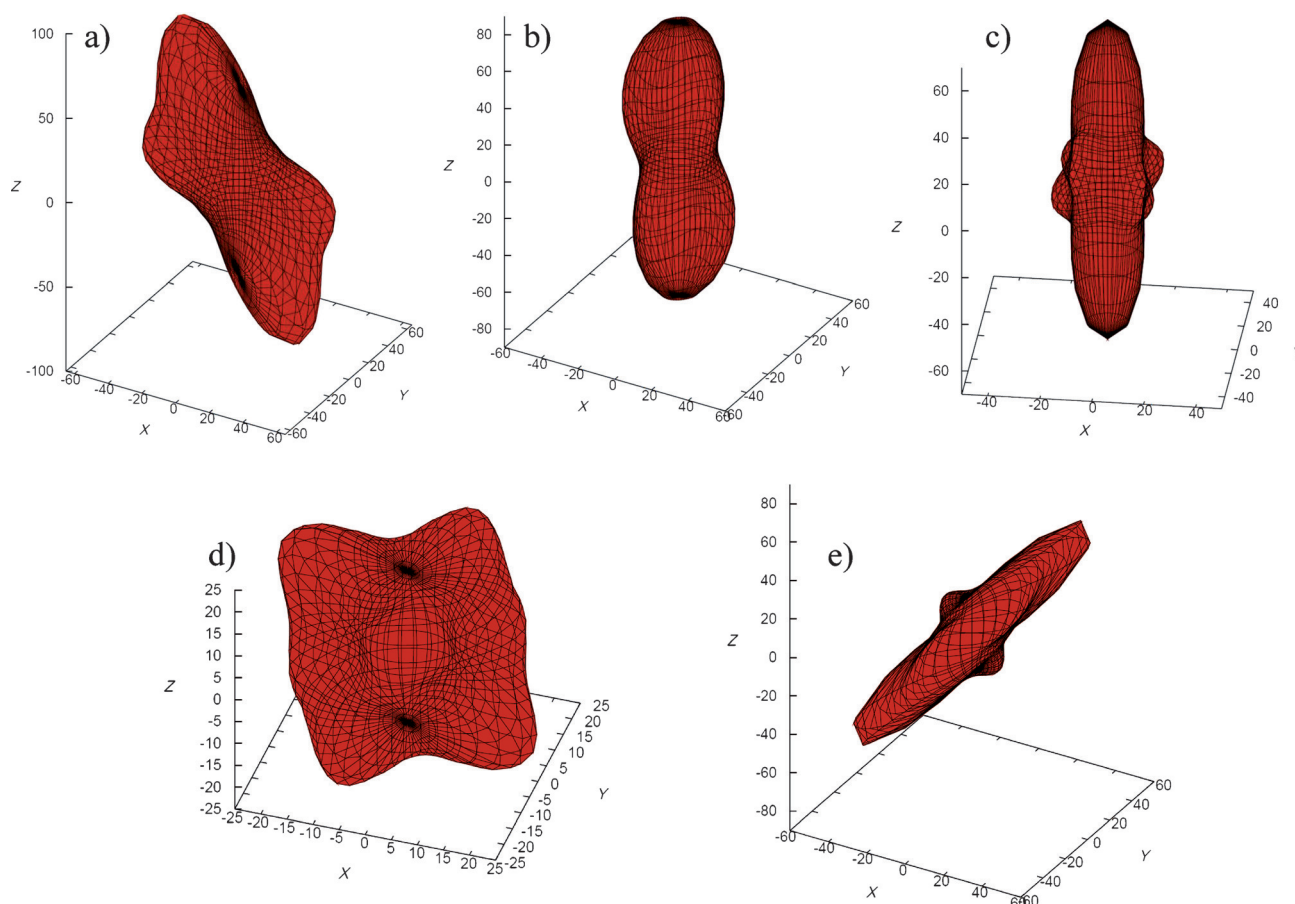


**Figure 2.** Computed three-dimensional rendering of Young's modulus of: a)  $\alpha$ -glycine, b)  $\gamma$ -glycine, c) L-alanine, d) DL-serine, and e) glycyglycine. Each plot features a two-dimensional surface, constructed by setting the distance from the origin of each point on the surface to the value of Young's modulus in the direction of the vector pointing from the origin to that point. Therefore, the axes are given in GPa and negative signs indicate direction only. Lattice vectors have been aligned following the convention of  $\vec{x} \parallel \vec{a}$ ,  $\vec{z} \parallel (\vec{a} \times \vec{b})$ .<sup>[50,51]</sup>

tion from the underlying hydrogen-bond network to the mechanical stiffness. Furthermore, we find that Young's modulus values are usually highly anisotropic, as they depend on the relative orientation between the crystal facet and the hydrogen-bond network directions. In fact, we predict theoretically that these values could be twice or three times as large as the observed values if special facet orientations can be stabilized. This opens a route to rational design of ultra-stiff materials based on molecular solids.

### Experimental Section and Methods

Pure crystals of  $\alpha$ -glycine (Alfa Aesar 99.5+%), glycyglycine (Apollo Scientific 99%), L-alanine (Sigma 98%), and DL-serine (Alfa Aesar 99%) were grown by a slow evaporation technique from aqueous solutions at 23 °C, in a clean-room environment. The  $\gamma$ -glycine crystals were obtained by growing glycine in the presence of 15% (w/w)  $\text{ZnCl}_2$ . Large transparent single crystals (shown as insets in Figure 1) were chosen, washed with pure Millipore water, and dried with filter paper. The packing arrangements were verified and the major faces were indexed with an Ultima III (sealed X-ray tube, Cu anode, 3 kW, RIGAKU, Japan) X-ray diffractometer.

Mechanical characteristics were measured using an Agilent XP nanoindenter, equipped with a Berkovich indenter tip. Typically, 12–16 separate indentations were performed on three different crystals.

The tip was loaded into the sample at a strain rate of  $0.05 \text{ s}^{-1}$ , until the ultimate depth of 800 nm was reached (at 15–20 mN load). The Young modulus,  $E$ , and nanohardness,  $H$ , were recorded continuously during the loading using continuous stiffness measurement. The latter imposed a small (2 nm) modulation on the quasi-static load, allowing continuous reading of both  $E$  and  $H$  as the load on the sample was increased.  $E$  and  $H$  for each test were taken as their average between depths of 350 to 700 nm. The tip area function was determined by calibration on a fused quartz sample, with  $E$  calculated by the Oliver–Pharr technique.<sup>[10]</sup> From the DFT calculation, Voigt and Reuss averaged Poisson ratios<sup>[41]</sup> are between 0.27 and 0.36 for all amino acid crystals studied. Therefore, a Poisson ratio of 0.3 was assumed for all measurements. Strictly, this technique applies to isotropic materials. Computational techniques for treatment of anisotropic materials<sup>[44,45]</sup> would only affect results for some of the crystal faces and not change the observed qualitative trends.

All calculations were performed using the generalized gradient approximation (GGA) exchange-correlation functional of Perdew, Burke, and Ernzerhof (PBE),<sup>[46]</sup> augmented by Tkatchenko–Scheffler dispersive pairwise-correction corrections.<sup>[47]</sup> Details of the Brillouin zone sampling are given in the Supporting Information. The total energy was converged to  $10^{-7}$  eV per unit cell in all calculations and all forces in the optimized structures were smaller than  $5 \times 10^{-3} \text{ eV \AA}^{-1}$ , with the stress optimized to better than the ratio between the minimal force and the lattice face area.

All calculations were performed using VASP,<sup>[48]</sup> a projector-augmented planewave code, with a high energy planewave cutoff of

950 eV, needed to obtain converged stress calculations. Young's moduli were then computed based on the method of Wu et al.<sup>[43]</sup> and further verified against explicit energy-strain calculations<sup>[49]</sup> for  $\alpha$ -glycine (see the Supporting Information for details).

## Acknowledgements

This work has been supported by the Deutsch-Israelische Projektkooperation (DIP) program, the Lise Meitner Minerva Center for Computational Chemistry, the Israel Science Foundation, the Gerhard Schmidt Center for Supramolecular Structures at the Weizmann Institute, and the historic generosity of the Perlman family. I.A. wishes to thank Asaf Azuri (Weizmann Institute), Isabelle Weissbuch (Weizmann Institute), Ashwin Ramasubramaniam (University of Massachusetts), and Per Söderlind (Lawrence Livermore National Lab) for helpful discussions. A.M.R. acknowledges the support of the US Office of Naval Research, under Grant N00014-14-1-0761. Part of this research was conducted while A.M.R. was on sabbatical at the Weizmann Institute of Science. The sabbatical period was supported by a grant from the Weston Visiting Professorship Program.

**Keywords:** amino acids · crystallography · density functional calculations · mechanical properties · Young's modulus

**How to cite:** *Angew. Chem. Int. Ed.* **2015**, *54*, 13566–13570  
*Angew. Chem.* **2015**, *127*, 13770–13774

- [1] N. Kol, L. A. Abramovich, D. Barlam, R. Z. Shneck, E. Gazit, I. Rouso, *Nano Lett.* **2005**, *5*, 1343–1346.
- [2] L. Niu, X. Chen, S. Allen, S. J. B. Tendler, *Langmuir* **2007**, *23*, 7443–7446.
- [3] J. D. Bauer, E. Haussühl, B. Winkler, D. Arbeck, V. Milman, S. Robertson, *Cryst. Growth Des.* **2010**, *10*, 3132–3140.
- [4] K. J. Ramos, D. E. Hooks, D. F. Bahr, *Philos. Mag.* **2009**, *89*, 2381–2402.
- [5] K. J. Ramos, D. F. Bahr, D. E. Hooks, *Philos. Mag.* **2011**, *91*, 1276–1285.
- [6] S. C. Sahoo, S. B. Sinha, M. S. R. N. Kiran, U. Ramamurty, A. F. Dericioglu, C. M. Reddy, P. Naumov, *J. Am. Chem. Soc.* **2013**, *135*, 13843–13850.
- [7] G. R. Krishna, M. S. R. N. Kiran, C. L. Fraser, U. Ramamurty, C. M. Reddy, *Adv. Funct. Mater.* **2013**, *23*, 1422–1430.
- [8] N. K. Nath, M. K. Panda, S. C. Sahoo, P. Naumov, *CrystEngComm* **2014**, *16*, 1850–1858.
- [9] M. K. Panda, S. Ghosh, N. Yasuda, T. Moriwaki, G. D. Mukherjee, C. M. Reddy, P. Naumov, *Nat. Chem.* **2015**, *7*, 65–72.
- [10] W. C. Oliver, G. M. Pharr, *J. Mater. Res.* **2004**, *19*, 3–20.
- [11] H. J. Butt, B. Cappella, M. Kappl, *Surf. Sci. Rep.* **2005**, *59*, 1152.
- [12] S. Varughese, M. S. R. N. Kiran, U. Ramamurty, G. R. Desiraju, *Angew. Chem. Int. Ed.* **2013**, *52*, 2701–2712; *Angew. Chem.* **2013**, *125*, 2765–2777.
- [13] U. Ramamurty, J. I. Jang, *CrystEngComm* **2014**, *16*, 12–23.
- [14] A. M. Reilly, A. Tkatchenko, *Phys. Rev. Lett.* **2014**, *113*, 055701.
- [15] S. Karki, T. Friščić, L. Fábíán, P. R. Laity, G. M. Day, W. Jones, *Adv. Mater.* **2009**, *21*, 3905–3909.
- [16] S. Ghosh, A. Mondal, M. S. R. N. Kiran, U. Ramamurty, C. M. Reddy, *Cryst. Growth Des.* **2013**, *13*, 4435–4441.
- [17] I. Azuri, L. A. Abramovich, E. Gazit, O. Hod, L. Kronik, *J. Am. Chem. Soc.* **2014**, *136*, 963–969.
- [18] K. J. Ramos, D. F. Bahr, *J. Mater. Res.* **2007**, *22*, 2037–2045.
- [19] S. G. Gevorkyan, *Biophysics* **1990**, *35*, 393–394.
- [20] J. C. A. Boeyens, J. F. Ogilvie, *Molecules, Mysteries and Magic of Molecules*, Springer, Dordrecht, **2008**.
- [21] E. V. Boldyreva, S. N. Ivashevskaya, H. Sowa, H. Ahsbahs, H.-P. Weber, *Dokl. Akad. Nauk* **2004**, *396*, 358–361.
- [22] V. A. Drebuschak, E. V. Boldyreva, Y. A. Kovalevskaya, I. E. Paukov, T. N. Drebuschak, *J. Therm. Anal. Calorim.* **2005**, *79*, 65–70.
- [23] E. V. Boldyreva, S. N. Ivashevskaya, H. Sowa, H. Ahsbahs, H.-P. Weber, *Z. Kristallogr.* **2005**, *220*, 50–57.
- [24] S. V. Goryainov, E. N. Kolesnik, E. V. Boldyreva, *Physica B* **2005**, *357*, 340–347.
- [25] C. Murli, S. M. Sharma, S. Karmakar, S. K. Sikka, *Physica B* **2003**, *339*, 23–30.
- [26] J. Staun Olsen, L. Gerward, A. G. Souza Filho, P. T. C. Freire, J. Mendes Filho, F. E. A. Melo, *High Pressure Res.* **2006**, *26*, 433–437.
- [27] K. Rajesh, P. P. Kumar, *J. Mater.* **2014**, 790957.
- [28] S. Tamilselvan, M. Vimalan, I. V. Potheher, S. Rajasekar, R. Jeyasekaran, M. A. Arockiaraj, J. Madhavan, *Spectrochim. Acta Part A* **2013**, *114*, 19–26.
- [29] R. J. Roberts, R. C. Rowe, P. York, *Powder Technol.* **1991**, *65*, 139–146.
- [30] S. Varughese, M. S. R. N. Kiran, U. Ramamurty, G. R. Desiraju, *Chem. Asian J.* **2012**, *7*, 2118–2125.
- [31] S. Shankar, R. Balgley, M. Lahav, S. R. Cohen, R. Popovitz-Biro, M. E. van der Boom, *J. Am. Chem. Soc.* **2015**, *137*, 226–231.
- [32] A. P. J. Middelberg, L. He, A. F. Dexter, H. H. Shen, S. A. Holt, R. K. Thomas, *J. R. Soc. Interface* **2008**, *5*, 47–54.
- [33] J. Klimeš, A. Michaelides, *J. Chem. Phys.* **2012**, *137*, 120901.
- [34] S. Grimme, J. Antony, S. Ehrlich, H. Krieg, *J. Chem. Phys.* **2010**, *132*, 154104.
- [35] K. E. Riley, M. Pitoňák, P. Jurečka, P. Hobza, *Chem. Rev.* **2010**, *110*, 5023–5063.
- [36] L. Kronik, A. Tkatchenko, *Acc. Chem. Res.* **2014**, *47*, 3208–3216, and references therein.
- [37] P. Langan, S. A. Mason, D. Myles, B. P. Schoenborn, *Acta Crystallogr. Sect. B* **2002**, *58*, 728–733.
- [38] R. Destro, R. E. Marsh, R. Bianchi, *J. Phys. Chem.* **1988**, *92*, 966–973.
- [39] A. F. Bower, *Applied Mechanics of Solids*, CRC, Boca Raton, US, **2009**.
- [40] J. F. Nye, *Physical Properties of Crystals: Their Representation by Tensors and Matrices*, Oxford University Press, Oxford, **1957**.
- [41] A. Marmier, Z. A. D. Lethbridge, R. I. Walton, C. W. Smith, S. C. Parker, K. E. Evans, *Comput. Phys. Commun.* **2010**, *181*, 2102–2115.
- [42] Y. L. Page, P. Saxe, *Phys. Rev. B* **2002**, *65*, 104104.
- [43] X. Wu, D. Vanderblit, D. R. Hamann, *Phys. Rev. B* **2005**, *72*, 035105.
- [44] J. G. Swadener, G. M. Pharr, *Philos. Mag.* **2001**, *81*, 447–466.
- [45] J. J. Vlassak, W. D. Nix, *J. Mech. Phys. Solids* **1994**, *42*, 1223–1245.
- [46] J. P. Perdew, K. Burke, M. Ernzerhof, *Phys. Rev. Lett.* **1996**, *77*, 3865–3868.
- [47] A. Tkatchenko, M. Scheffler, *Phys. Rev. Lett.* **2009**, *102*, 0730051.
- [48] G. Kresse, J. Furthmüller, *Comput. Mater. Sci.* **1996**, *6*, 15–50.
- [49] P. Söderlind, J. E. Klepeis, *Phys. Rev. B* **2009**, *79*, 104110.
- [50] R. Golezorkhtabar, P. Pavone, J. Spitaler, P. Puschnig, C. Draxl, *Comput. Phys. Commun.* **2013**, *184*, 1861–1873.
- [51] B. Militzer, H. R. Wenk, S. Stackhouse, L. Stixrude, *Am. Mineral.* **2011**, *96*, 125–137.

Received: June 25, 2015

Published online: September 16, 2015